PAPER • OPEN ACCESS

Projected flame length and flame extension length of horizontal buoyant jet flames

To cite this article: Nur Shahidah Ab Aziz and Rafiziana Md. Kasmani 2022 *J. Phys.: Conf. Ser.* **2259** 012027

View the article online for updates and enhancements.

Projected flame length and flame extension length of horizontal buoyant jet flames

Nur Shahidah Ab Aziz[1,2] and Rafiziana Md. Kasmani[2]

[1]School of Chemical Engineering, Universiti Teknologi MARA, Malaysia
[2]School of Chemical Engineering and Energy, Universiti Teknologi Malaysia, Malaysia

E-mail: rafiziana@utm.my

Abstract. Jet fires are a type of dangerous fire caused by the sudden release of flammable materials. In this work, propane was used as fuel and released through a 7.15mm and 9.8 mm circular nozzle with the exit velocities were set ranging between 27 and 65 m/s. The data of this study are compared against theoretical measurement and prediction using previously suggested correlation for projected flame length and flame extension length. It was determined, the projected flame length gives a good prediction by using theoretical measurement while for the prediction of flame extension length, an elliptical shape assumption was suitable to be used after impinging point for a horizontal buoyant jet fire.

Keywords: jet flame, impingement, horizontal, buoyant.

1. Introduction

Any industrial facility that works with pressurized pipelines and vessels is at risk of a jet fire. The presence of obstacles downstream might result in an impingement scenario and eventually, an accident escalation called domino effects. The behavior and intensity of the impingement scenario are depending on the jet direction and the geometric design of the system [1]. It was stated by Pula, et al. [2], jet fire in horizontal orientation poses a higher risk than in vertical orientation. A few provisions were done using empirical correlation, semi-empirical model, and simulation to estimate the geometrical flame features, radiant heat, and temperature distribution over a range of release scenarios of horizontal jet fire. However, scarce data is available on the prediction for a buoyant horizontal jet fire. Furthermore, there are difficulties in defining the standard scenario that would lead to accident escalation due to jet fire impingement from these types of fire. Due to the shear forces between the jet and the surrounding air, the issuing jet fire promotes air entrainment into a still atmosphere. The flame projection of a horizontal jet flame is different to that of a vertical jet flame in still air, in which the direction of momentum and buoyancy forces are in a similar direction for vertical jet flame while in horizontal jet flame, the direction is perpendicular with each other owing to gravitational forces and buoyancy [3].

As a result, the geometrical characteristics of horizontal jet flames should take into account both the projected flame length horizontally, L_p, and the projected flame height vertically, H_p [4]. The prediction of both parameters has been done by using theoretical prediction based on mass, momentum, and mixture fraction conservation equation [5, 6]. It was called a flame integral model. Other than prediction using a theoretical assumption of the flame integral model, Palacios, et al. [7] compiles a comprehensive

dataset of horizontal sonic and subsonic jet fire tests including numerous gas fuels and release circumstances. The suggested correlation was drawn based on the heat release rate, Q.

However, the said correlation is only limited to the free jet fire scenario. While there is no specific method to identify the L_p and H_p for impingement scenario of horizontal jet flames, a case of vertical jet flame impingement was taken as a basis to measure associated geometrical features for horizontal jet flames. In the impingement scenario of vertical jet flames, L_p was distributed axially on the surface and called flame extension length. Although the direction and geometry of the target shape are different in this study, a similar methodology was utilized to characterize the flame behavior as follows: (i) Projected flame height (Hp) is believed to be similar to radial displacement (r_f) in Kong, et al. [8] earlier's study, (ii) (c) For this investigation, vertical displacement in an upward and downward direction is assumed to be similar to radial displacement in an upward and downward direction for an inclined ceiling [8] or to left and right displacement for a level ceiling [9], (iii) In this investigation, the convex surface of the target item is believed to be comparable to a flat surface. By using these assumptions, the H_p and L_p were then analyzed.

In this study, You and Faeth [10] presented an empirical formula for predicting the flame extension length beneath the plate when the flame height to plate-source height ratio, $[(L_p-D)/d]$ was between 0 and 5.8. Other work focuses on thermal impinging flow produced by a strong buoyant plume and new correlations for predicting the length of the flame extension beneath the plate were suggested based on cylindrical or ellipse flame shape hypothesis [11]. Huang, et al. [12] is then used the same hypothesis to predict the flame extension length for a horizontal jet impinged on a vertical plate. However, additional data were required to demonstrate that the correlations hold for varying distances between the nozzle orifice and the vertical plate. Thus, this study aims to extend the validity of the said correlation to estimate the projected flame length, Lp, and the flame extension length, Hp once it impinged on a surface for a flame height to plate-source height ratio 20 to 110 which implies a larger scale of impingement release.

2. Methodology

An experimental setup was shown in Figure 1. The facility is comprised of a series of pressurized gas supply lines connected to a 1-meter horizontal pipe that serves as a stagnation chamber via a flexible high-pressure hose. The flow controller supplied by Alicat Scientific (MCR500) was used, along with a solenoid valve, which was installed along the nozzle line to allow gas release at the desired flow rate. To avoid backflow, a check valve was also installed at the flowmeter's input line for safety. The flow controller controlled the flow of hydrocarbons, which were ejected through 7.15-mm and 9.8-mm circular nozzles attached to the pipe to create a horizontal diffusion jet flame. The release nozzle is aligned to the center of the cylindrical vessel head to allow a jet fire impingement scenario.
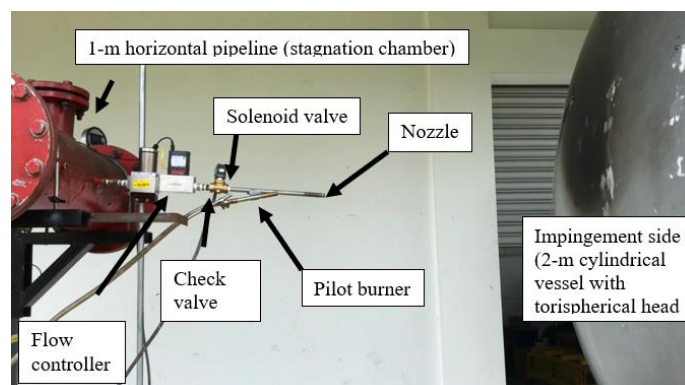

Figure 1. Experimental setup

2.1. Release conditions

The nominal experimental settings of the jet release for free and impinging situations are shown in Table 1 and Table 2.

Table 1. Nominal experimental conditions of free jet fire release

No test	Test name	Nozzle size, d (mm)	Mass flowrate, m (SLPM)	Camera position x, y, z (m,m,m)
1	JFF	9.8	80	0.3,3.7,0
2			120	
3			160	
4			200	0.4,3.7,0
5			250	
6			300	0.5,3.7,0

Table 2. Nominal experimental conditions of impinging jet fire

No test	Test name	Nozzle size, d (mm)	Release distance (m)	Mass flowrate, m (SLPM)	Camera position x,y,z (m,m,m)
1	JFI_9.8a	9.8	0.8	80	0.5,3.7,0
2				120	
3				160	
4				200	
5				250	
6				300	
7	JFI_9.8b		1.2	80	
8				160	
9				200	
10	JFI_7.15	7.15	0.8	200	
11				250	
12				300	

2.2. Image Processing

The raw photos were rendered from videos recorded at 100fps and further pre-processed with the MATLAB Image Processing Toolbox to extract the flame geometrical parameters, namely the projected flame length L_p and the projected flame height, H_p. The image processing technique was adapted from a prior study (1-5) which resulted in the following contour plot.
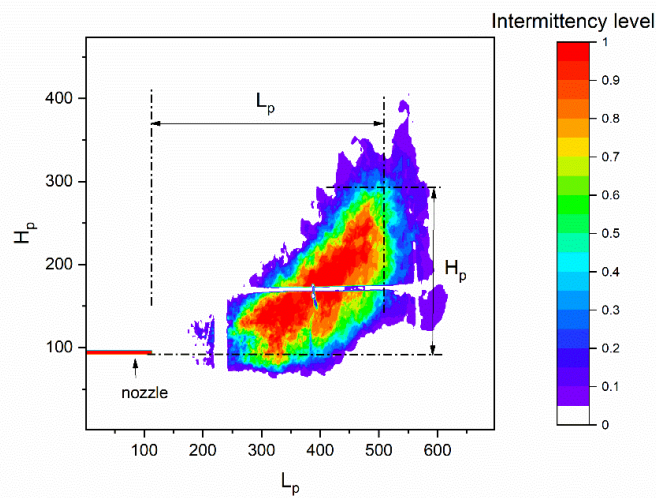
Figure 2. Flame appearance intermittency contour

2.3. Data Analysis

The main data obtained from this study are the geometrical flame features, L_p and H_p. The following theoretical correlation based on mass, momentum, and mixture fraction called flame integral model was used for the L_p and H_p prediction.

$$tan\theta = \frac{1}{\sqrt{\rho_0/\rho_\infty}Fr^*}\left[\left(\frac{s}{d}\right) + 2\beta\left(\frac{s}{d}\right)^2 + \frac{4}{3}\beta^2\left(\frac{s}{d}\right)^3\right]$$

(1)

The curvilinear coordinate system specifies s as the arc length along the jet centerline and θ as the jet angle perpendicular to the local jet centerline and measured with respect to the horizontal axis (x-axis). L_p and H_p were predicted using the angle, θ, and location of the curvilinear coordinate, s. Several other parameters were included, which are the jet density, ρ_0, ambient density, ρ_∞, modified Froude number,

$Fr^* = Fr\sqrt{\frac{\rho_0}{\rho_\infty}\frac{\rho_\infty}{\alpha_2(\rho_\infty - \rho_{st})}}$ and nozzle diameter d.

Other than prediction using theoretical assumption, Palacios, García (6) compiles a comprehensive dataset of horizontal sonic and subsonic jet fire tests including numerous gas fuels and release circumstances. A correlation for projected flame length was proposed which correlate dimensionless projected flame length (L_p/d) with dimensionless heat release rate, $\dot{Q}^* = \frac{Q}{c_p\rho_\infty T_\infty\sqrt{gd^5}}$ where d is the source diameter (m), ρ_∞ is the ambient density (kg.m^{-3}), T_∞ is the ambient temperature (K) and c_p is the specific heat of air at constant pressure (kJ^{-1} kg^{-1} K^{-1}). The proposed correlation was presented as follows

$$L_p/d = 3.7Q^{*0.35}$$

(2)

3. Results and Discussion

3.1. Experimental observation

In this study, the projected flame length (L_p) is defined as the distance between the nozzle exits and the furthest visible flame tip in the horizontal direction of the flame appearance intermittency contour with a 50% probability as depicted in Figure 2 (2). Most previous studies used L_p as a basis for radiant heat estimation using a semi-empirical model (7-10). The horizontal projected flame length is plotted versus the exit velocity, u_e, as shown in Figure 3.
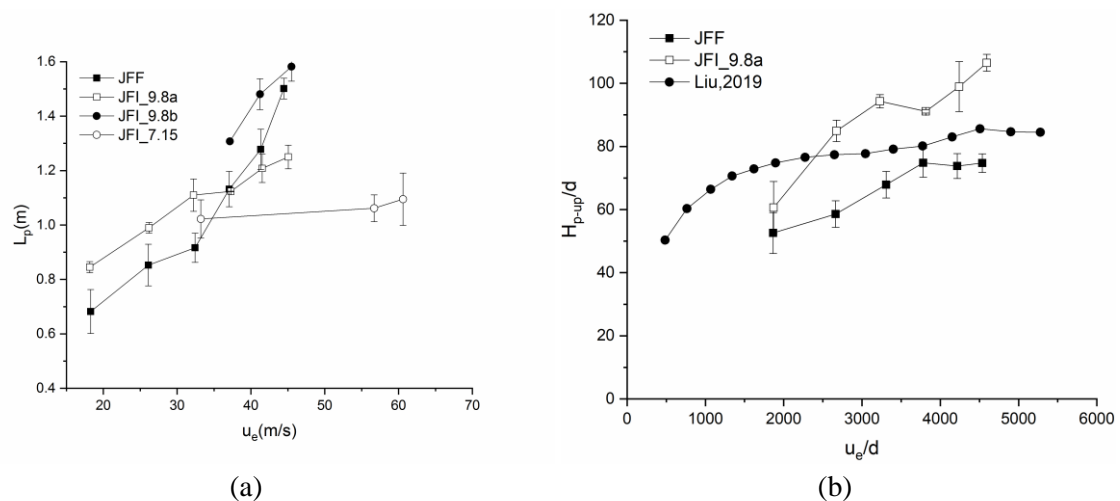

(a)   (b)

Figure 3. (a) Projected flame length against exit velocity (m/s) (b) Projected flame height at a variety of strain rates of free jet fire release and comparison with the previous study of Liu, Delichatsios (11).

The error bar indicates the repeatability of the test. For all release conditions, the flame length increases with exit velocity. However, when comparing JFI 7.15 to other release circumstances, the increment is not as visible. This is due to a higher exit velocity, more air is entrained which means more oxidizer is provided and combined with the released fuel and allows for more complete combustion. As a result, even when the released mass flow rate is increased, the resulting flame lengths are nearly identical in-between cases. Figure 3(a) further indicates that when the exit velocity is less than 37 m/s, the flame length grows in a similar pattern between the free jet fire scenario (JFF) and the impingement jet release scenario (JFI 9.8a).

However, a considerable difference can be seen when the velocity hits 37 m/s, with the increment of flame length being distinct for free jet fire release as opposed to the impingement scenario. The presence of an object/obstruction has deformed and dispersed the flame on the impinged surface, reducing the projected flame length. The flow's deceleration reduces the projected flame length. The data indicate strong agreement with JFF data for the impingement scenario with a higher nozzle to object separation distance of 1.2 m, implying that the effects of impingement are not as noticeable as at a smaller separation distance of 0.8 m. When the impinging jet fire was conducted at a greater separation distance, a greater L_p was observed at a lower exit velocity. The L_p, on the other hand, approaches free jet fire release as the velocity increases.

For the flame extension length, H_p, the findings for JFF show a good agreement with the earlier result of Liu, Delichatsios (11) as presented in Figure 3(b), where the jet flame height increased at first and then reduced later as the exit velocity increases. However, with an impingement situation (JFI 9.8a), the circumstance is different in which the flame height keeps growing as the release velocity

increased. As the flame impinged on the surface, the flame turned radially upwards and downward. The length of the upward and downward radial displacement was dictated by the release momentum.

3.2. Prediction using theoretical measurement

Figure 4 (a-b) plotted prediction of projected flame length, L_p and flame extension length, H_p using Eq (1) against measured data of experimental observation as plotted in Figure 3(a-b). As can be seen in Figure 4 (a), the projected flame length, L_p gives a comparable value of predicted against the measured value. However, the projected flame height, H_p as shown in Figure 4 (b), scattered data was observed which shows overprediction for release nozzle of 7.15 mm (JFI_7.15) and underprediction for release nozzle of 9.8 mm (JFI_9.8a and JFI_9.8b). Furthermore, it shows the inconsistency of prediction for free jet fire release (JFF). This is mainly due to the assumption used in the theoretical measurement of the flame features as presented in Eq (1) which does not consider the effects of impingement particularly the separation distance.
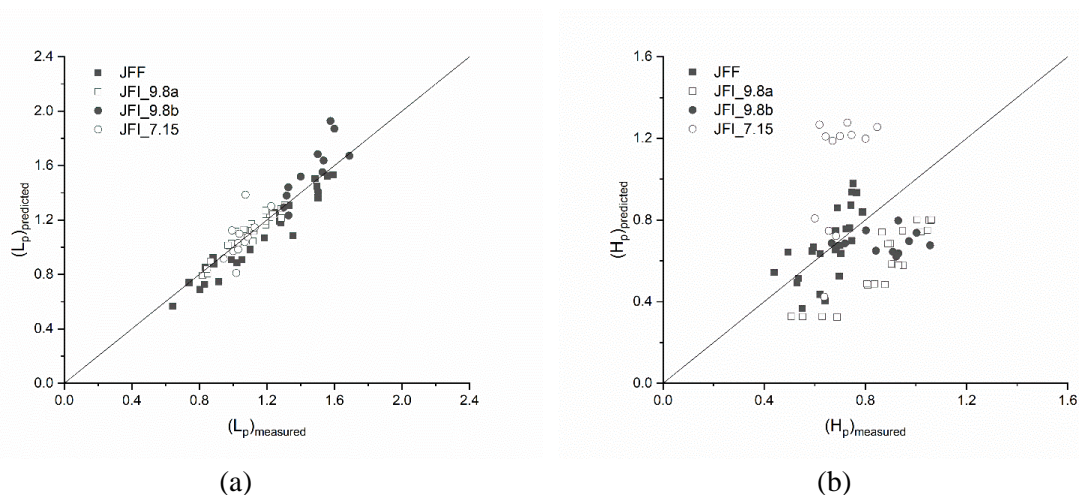

(a)   (b)

Figure 4. (a) Comparison of predicted and measure value of L_p (b) Comparison of predicted and measure value of H_p.

3.3. Comparison against previous correlation

3.3.1. Projected flame length. The data from this investigation were then compared to those from a prior study by Palacios, García (6) for free horizontal jet flames by using the following proposed equation. The graph of measured data against predicted L_p was plotted as in Figure 5.

$$L_p/d = 3.7Q^{*0.35} \tag{3}$$

The data appears to diverge more significantly in the case of free jet fire release (**Figure 5**(a)) at low release velocity than in any other impingement scenario. This is because of a buoyancy-driven condition that leads the flame to bend upward to achieve a lower release velocity. The turbulent diffusion flame is generally coupled to the nozzle at a sufficiently low exit velocity (12). As a result, gravity forces were less effective, which may have resulted in more vertical displacement at lower release values. Another possible explanation is that the subsonic release produced in this work ($Q^* <$

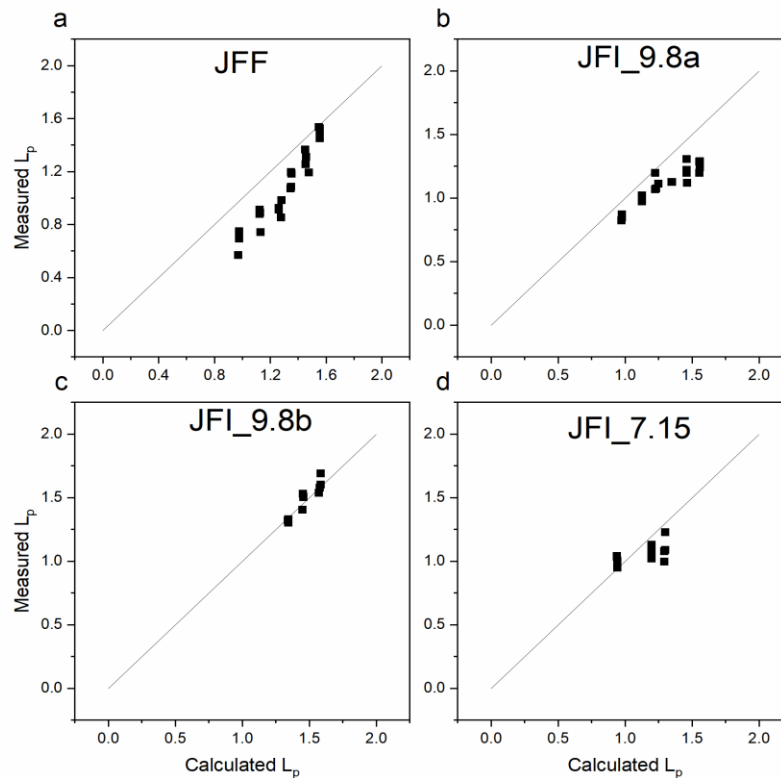10^5) is consistent with Zukoski, Kubota (13), although the equation derived is for sonic release.

Figure 5. Prediction of projected flame length for all release scenarios (a) JFF (b) JFI_9.8a (c)JFI_9.8b and (d)JFI_7.15.

3.3.2. Flame extension length. Numerous correlations were proposed for the flame length beneath the impinging jet fire's ceiling. To our knowledge, the only literature on jet flame impingement is on horizontal ceilings (either flat or concave). In this study, the target object's convex surface is assumed to be similar to a flat surface. The flame extension before the impingement site is quantified physically by the amount of unburned fuel remaining after impingement and the amount of unburned fuel consumed during transit along the imping surface. Eq (4) represents the relationship between the flame height and the volume of unburned fuel after the impingement point (14).

$$\frac{H_p}{D} \sim fcn\left(\frac{V_{fu}}{V_f}\dot{Q}\right) \tag{4}$$

where H_p is the flame extension length, D is the nozzle-to-object separation distance, V_{fu} is the flame volume portion intercepted by the imping surface in m^3, and V_f is the volume of the free flame in m^3. The flame volume intercepted by the imping surface can be represented by the flame geometry such as cylinder and ellipse for the vertical jet fire on a horizontal and inclined surface (14-17). The following

Eq(5)-(6) correlate the upward flame height after impingement points for cylindrical and elliptical flame shapes, respectively.

$$\frac{H_p}{d} \sim \frac{1}{2}\left[\frac{(L_{p-free} - D)u_e}{L_{p-free}\sqrt{gD}}\right]^{1/2} \tag{5}$$

$$\frac{H_p}{d} \sim \left[\frac{[\frac{1}{9}L_{p-free}^{3} - (\frac{1}{3}D^3 ln\frac{L_{p-free}}{D} + \frac{1}{9}D^3)]u_e}{\frac{1}{9}L_{p-free}^{3}\sqrt{gD}}\right]^{1/2} \tag{6}$$

Based on these comparable assumptions and the plotted graph of different flame shape assumptions after the impinging point, the following deduction was made, in which elliptical shape was suitable to be used with $R^2=0.97$, a slightly higher than by using cylindrical flame shape assumption with $R^2=0.95$ to estimate the projected flame height after the impinging point.
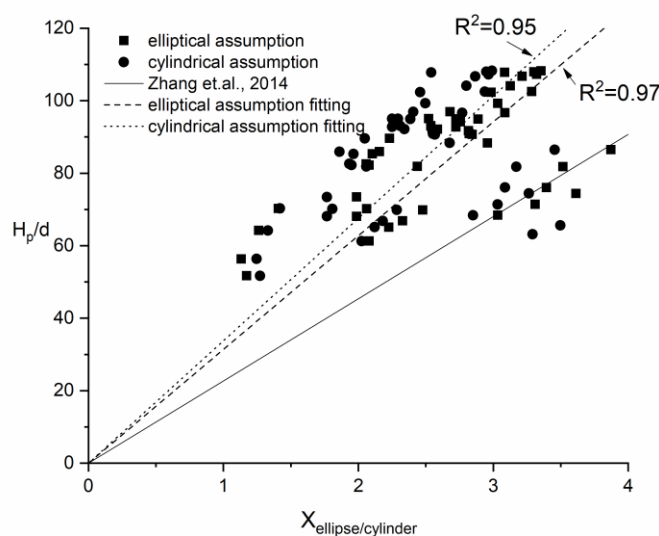

Figure 6. Non-dimensional correlation of upward flame extension height on an impinged surface based on cylindrical and elliptical flame shape.

4. Conclusion

In this study, a correlation was proposed for the prediction of projected flame length, Lp and projected flame height, Hp for different jet release scenarios; free and impinging jet. The main conclusion is as follows;

a) By employing the previously proposed correlation by Palacios, García (6) for projected flame length, the measured data were well correlated for higher momentum in free jet fire release scenario and lower

momentum

b) The projected flame height trend was consistent with earlier data. The correlation of flame height was computed based on the flame volume intercepted at the impinged location using the assumption of identical observations acquired from jets impinged vertically on inclined/horizontal ceilings. It was observed, the elliptical flame shape assumption provides a better fit than the cylindrical flame form assumption.

As a recommendation for future work, more data of horizontal jet fire impingement scenario based on different variables i.e nozzle shape and shape of the impinging surface will be needed to extend the applicability of the equation on L_p and H_p proposed.

Acknowledgment

References

[1] Laboureur DM, Gopalaswami N, Zhang B, Liu Y, Mannan MS. 2016 Experimental study on propane jet fire hazards: Assessment of the main geometrical features of horizontal jet flames *Journal of Loss Prevention in the Process Industries* **41** 355-64.

[2] Zhou K, Wang Y, Zhang L, Wu Y, Nie X, Jiang J. 2020 Effect of nozzle exit shape on the geometrical features of horizontal turbulent jet flame *Fuel* **260**.

[3] Gonzalez RC, Woods RE, Eddins SL. Digital Image Processing Using MATLAB. 2nd ed. United States of America: Gatesmark Publishing; 2009.

[4] Liu J, Wang J, Chen M. 2019 Estimating the trajectory length of buoyant turbulent jet flames issuing from a downward sloping nozzle *Process Safety and Environmental Protection* **132** 153-9.

[5] Ab Aziz NS, Kasmani RM, Samsudin MDM, Ahmad A. 2020 Main geometrical features of horizontal buoyant jet fire and associated radiative fraction *Process Safety Progress* **39** e12124.

[6] Palacios A, García W, Rengel B. 2020 Flame shapes and thermal fluxes for an extensive range of horizontal jet flames *Fuel* **279** 118328.

[7] Zhou K, Jiang J. 2016 Thermal Radiation From Vertical Turbulent Jet Flame: Line Source Model *Journal of Heat Transfer* **138**(4) 042701.

[8] Zhou K, Liu J, Jiang J. 2016 Prediction of radiant heat flux from horizontal propane jet fire *Applied Thermal Engineering* **106** 634-9.

[9] Bradley D, Gaskell PH, Gu X, Palacios A. 2016 Jet flame heights, lift-off distances, and mean flame surface density for extensive ranges of fuels and flow rates *Combustion and Flame* **164** 400-9.

[10] Palacios A, Munoz M, Darbra RM, Casal J. 2012 Thermal radiation from vertical jet fires *Fire Safety Journal* **51** 93-101.

[11] Liu S, Delichatsios MA, Hu L. 2019 Flame profile parameters of horizontal turbulent jets: Experiments, similarity analysis and an integral model *Combustion and Flame* **207** 1-9.

[12] Wang Z, Zhou K, Zhang L, Nie X, Wu Y, Jiang J, et al. 2021 Flame extension area and temperature profile of horizontal jet fire impinging on a vertical plate *Process Safety and Environmental Protection* **147** 547-58.

[13] Zukoski EE, Kubota T, Cetegen B. 1981 Entrainment in fire plumes *Fire safety journal* **3**(2) 107-21.

[14] Zhang X, Tao H, Xu W, Liu X, Li X, Zhang X, et al. 2017 Flame extension lengths beneath an inclined ceiling induced by rectangular-source fires *Combustion and Flame* **176** 349-57.

[15] Qiu A, Hu L, Chen L, Carvel RO. 2018 Flame extension lengths beneath a confined ceiling induced

by fire in a channel with longitudinal air flow *Fire Safety Journal* **97** 29-43.

[16] Zhang X, Hu L, Delichatsios MA, Zhang J. 2019 Experimental study and analysis on flame lengths induced by wall-attached fire impinging upon an inclined ceiling *Proceedings of the Combustion Institute* **37**(3) 3879-87.

[17] Zhang X, Hu L, Zhu W, Zhang X, Yang L. 2014 Flame extension length and temperature profile in thermal impinging flow of buoyant round jet upon a horizontal plate *Applied Thermal Engineering* **73**(1) 15-22.